2023 62nd IEEE Conference on Decision and Control (CDC)
December 13-15, 2023. Marina Bay Sands, Singapore

Observer-based Output Feedback Stabilization for Stop–and–Go Waves of Vehicle Traffic Flow

Haoran Luan, Jingyuan Zhan, Xiaoli Li, Liguo Zhang

Abstract— **This paper designs an observer–based output feedback controller for traffic flow with stop–and–go waves and disturbances in order to dissipate traffic congestion. The macroscopic traffic flow dynamics in the congestion regime is described by the linearized Aw–Rascle–Zhang (ARZ) traffic flow model over a time–varying moving spatial domain, and according to the Rankine–Hugoniot condition and the characteristic velocities of the ARZ model, a novel propagation model of the stop–and–go waves is proposed. To stabilize the traffic state and the stop–and–go waves, and to suppress traffic disturbances, an observer–based output feedback controller is designed by using the PDE backstepping method. The controller utilizes the estimated state of an observer, which is constructed based on boundary measurements only. The exponential stability of the closed–loop system in the H^1 norm is proved by the Lyapunov analysis. Finally, the effectiveness of the controller for stabilizing the traffic state with stop–and–go waves and disturbances is verified by numerical simulations.**

I. INTRODUCTION

Traffic flow may become instable and lead to stop–and–go waves due to delays in drivers adapting their speed to traffic conditions. Different traffic states exist on both sides of the stop–and–go waves, which can result in discontinuous traffic speeds and densities at the interface [1]. A famous experiment in Japan on a circular road demonstrated that stop–and–go waves could still emerge and propagate backwards even when drivers tried to avoid them [2]. At present, studying the stabilization of stop–and–go waves by uncovering their propagation dynamics has become one of the most fundamental issues in the field. The goal is to mitigate congestion and improve traffic efficiency.

Among the extensive studies for traffic congestion mitigation, hyperbolic Partial Differential Equations (PDEs) are commonly used to describe traffic flow systems. The second–order Aw–Rascle–Zhang (ARZ) model [3] is a non–equilibrium traffic flow model that describes the changing rate of vehicle speed. This allows for a more accurate characterization of the formation, propagation, and dissipation of stop–and–go waves. In [4], an output feedback boundary controller based on the extended ARZ models was designed for the two–lane traffic flow. Using the Backstepping method, an output feedback control law was developed in [5] in order to damp out traffic stop–and–go waves in the congested regime of the linearized two–class ARZ traffic model.

The effectiveness of controller on freeways heavily depends on accurate measurement of the traffic state. As such, traffic state estimation plays a crucial role in traffic control and management. [6] constructed an observer–based output feedback controller for the ARZ model to guarantee the integral input–to–state stability of the closed–loop system. [7] developed a distributed consensus–based boundary observer for freeway traffic flow network based on the linear ARZ model. [8] developed a boundary observer for estimation of congested freeway traffic states based on ARZ model.

However, the above studies are all within the fixed spatial domain. To the best of our knowledge, the investigation of control and estimation for ARZ traffic flow models based on time–varying moving spatial domains is limited. A bilateral boundary predictor feedback controller based on ARZ model was designed in [9] to stabilize the moving shock waves in congested traffic. Recently, we proposed a moving boundary observer based on ARZ model to estimate traffic flow state in [10]. In this paper, we study the moving boundary observer and full–state feedback controller design problem for traffic flow state with stop–and–go waves.

First, the macroscopic traffic flow dynamics in the congestion regime is described by the linearized ARZ model. Based on the Rankine–Hugoniot condition and the conservative condition of the ARZ model, the moving dynamics of the stop–and–go wave as a moving boundary is firstly described by means of the deviation of characteristic velocities before and after the shock wave. Moreover, we construct an observer system from boundary output measurement errors to estimate traffic state. Then, we employ the PDE backstepping method to obtain an observer–based output feedback controller. The exponential stability of the closed–system in the H^1 norm is proved via Lyapunov analysis. Finally, the validity of the controller is verified by numerical simulations.

This paper is organized as follows. The problem is described in Section II. The moving boundary observer is designed in Section III. The controller is constructed and the exponential stability of the closed–system is proved in Section IV. In Section V, numerical simulations are provided. Some conclusions are presented in Section VI.

Notation: We define u_t and u_x stand for the partial derivatives of the function u with respect to t and x, respectively. $u(x^-,t)$ and $u(x^+,t)$ stand respectively for the left and right trace, with respect to the variable x, of u at the point (x,t),

This work was supported by the National Natural Science Foundation of China (Nos. U2233211, 62273014), R&D Program of Beijing Municipal Education Commission (Nos. 23JD0020, KM202310005032), the Beijing Nova Program (No. 20220484133), the Beijing Municipal College Faculty Construction Plan for Outstanding Young Talents (No. BPHR202203011).

H. Luan, J. Zhan, X. Li and L. Zhang (corresponding author) are with the Faculty of Information Technology, Beijing University of Technology, and with the Beijing Key Laboratory of Computational Intelligence and Intelligent Systems, Beijing, 100124, China. (E-mail: luanhaoran@emails.bjut.edu.cn, jyzhan@bjut.edu.cn, lixiaolibjut@bjut.edu.cn, zhangliguo@bjut.edu.cn)

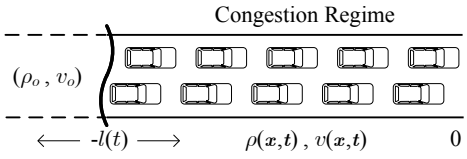

Fig. 1. Traffic flow in a congestion regime on $[-l(t),0]$.

i.e., $u(x^-,t)=\lim_{s\to x^-}u(s,t)$, $u(u^+,t)=\lim_{s\to x^+}u(s,t)$. For simplicity, $u(-l(t)^+,t)$ is represented by $u(-l(t),t)$ in this paper. $H^1((-l_0,0);\mathbb{R}^n)$ is the Sobolev space with initial location of stop–and–go wave $-l_0=-l(t_0)$ at the initial time t_0, and $||u(\cdot,t)||^2_{H^1_{((-l_0,0);\mathbb{R}^n)}}=\int_{-l(t)}^0 u^2(x,t)+u_x^2(x,t)dx$.

II. Problem Formulation

Consider the traffic flow state for a congestion regime on a stretch of freeway as shown in Fig. 1, where the left boundary of the congestion regime is movable due to the existence of a moving stop–and–go wave. And the left side of the stop–and–go wave is free–flow regime, which has a steady–state (ρ_o,v_o). The macroscopic traffic flow dynamic in congestion regime is described by the quasi–linear hyperbolic second–order ARZ model:

$$\rho_t+v\rho_x+\rho v_x=0, \tag{1}$$

$$v_t+(v-\rho\dot{p}(\rho))v_x=\frac{V(\rho)-v}{\tau}, \tag{2}$$

where $t\in[0,\infty)$, $x\in[-l(t),0]$. $v(x,t)$ is the average speed, $\rho(x,t)$ is the vehicle density. $-l(t)\in C^1(0,\infty)$ is the location of the stop–and–go waves, and $-L\le -l(t)\le 0$, with L being the length of the freeway. In [3], the traffic pressure term $p(\rho)$ is an increasing function w.r.t the density, which is given by $p(\rho)=v_f-V(\rho)=a\rho$, with $a=\frac{v_f}{\rho_m}$. $V(\rho)=v_f(1-\frac{\rho}{\rho_m})$ is Greenshields speed–density model of [11], ρ_m is the maximal density, and v_f is the free speed. τ is the relaxation term related to the driving behavior.

Letting $w(x,t)=v(x,t)+a\rho(x,t)$, then the ARZ model (1)–(2) can be described under the Riemann coordinate as

$$v_t-(w-2v)v_x=\frac{v_f-w}{\tau}, \tag{3}$$

$$w_t+vw_x=\frac{v_f-w}{\tau}, \tag{4}$$

where the characteristic eigenvalues (also called characteristic velocities) of the system are denoted by $\lambda_1=v$, $\lambda_2=-(w-2v)$.

We assume that system (3)–(4) is strictly hyperbolic, i.e. $\lambda_1>0$, and $\lambda_2\neq 0$. It is also assumed $\lambda_2<0$, which indicates that the speed information of traffic flow propagates from downstream to upstream, and the system lies in the congestion regime. And it usually leads to the stop–and–go wave phenomenon.

The propagation velocity of the stop–and–go wave $-\dot{l}(t)$ is derived based on Rankine–Hugoniot condition (see [12]), which ensure that the mass of the traffic flow is conserved at the moving interface. Since the density and flux before and after the stop–and–go wave are discontinuous, the stop–and–go wave can move along the freeway. We assume that there is only one stop–and–go wave presenting in the spatial domain, and thus we have

$$-\dot{l}(t)=\frac{q(-l(t)^-,t)-q(-l(t),t)}{\rho(-l(t)^-,t)-\rho(-l(t),t)}. \tag{5}$$

where $q(x,t)=\rho(x,t)v(x,t)$ is the traffic flux.

Proposition 1: *The propagation velocity of the stop–and–go wave is given by*

$$-\dot{l}(t)=\frac{2v(-l(t),t)-w(-l(t),t)}{2}+\frac{2v_o-w_o}{2}, \tag{6}$$

where $w(x,t)=v(x,t)+a\rho(x,t)$, $w_o=v_o+a\rho_o$.

Proof: Based on the Riemann conservation law of the ARZ model from [3], $w(-l(t),t)=w(-l(t)^-,t)$, $q(-l(t)^-,t)=q_o$, we have

$$\begin{aligned}-\dot{l}(t)=&\frac{q_o-q(-l(t),t)}{\rho_o-\rho(-l(t),t)}\\ =&\frac{a\rho(-l(t),t)(v_o-v(-l(t),t))-v_o(v_o-v(-l(t),t))}{v(-l(t),t)-v_o}\\ =&\frac{\lambda_2(-l(t),t)+v_o-a\rho_o}{2}\\ =&\frac{2v(-l(t),t)-w(-l(t),t)}{2}+\frac{2v_o-w_o}{2}.\end{aligned} \tag{7}$$

This concludes the proof of Proposition 1. □

Proposition 1 indicates that the propagation of the stop–and–go wave is determined only by the second characteristic velocity $\lambda_2=2v-w$ of ARZ model. When $-\dot{l}>0$, the stop–and–go wave moves downstream, and when $-\dot{l}<0$, it moves upstream.

In order to alleviate the traffic congestion, regulate traffic states and the stop–and–go wave, we design the velocity controller $U(t)$ at the downstream boundary $x=0$, thus we have boundary condition at $x=0$

$$v(0,t)=U(t)+d, \tag{8}$$

where $d\in\mathbb{R}$ is actuator input disturbances at the boundary.

To regulate the traffic flow dynamics around the constant steady–state (v^*,ρ^*) in congestion regime. Define the deviations the state $\bar{v}=v-v^*$ and $\bar{\rho}=\rho-\rho^*$, with $\bar{w}=w-w^*$, then we have the linearized ARZ model as

$$\bar{v}_t-(\omega^*-2v^*)\bar{v}_x=\frac{v_f-\bar{\omega}}{\tau}, \tag{9}$$

$$\bar{\omega}_t+v^*\bar{\omega}_x=\frac{v_f-\bar{\omega}}{\tau}. \tag{10}$$

Letting $-\bar{l}=-l-(-l^*)$, with the constant steady–state $-l^*$, the propagation velocity of the stop–and–go wave (6) is rewritten for the linearized ARZ model (9)–(10),

$$-\dot{\bar{l}}(t)=\frac{w^*}{2v^*}\bar{v}(-l(t),t). \tag{11}$$

Consider flux conservation law $\rho(-l(t),t)v(-l(t),t)=q(-l(t),t)$ at the upstream boundary $x=-l(t)$. Then we have the following boundary condition for system (9)–(10):

$$\bar{v}(0,t)=U(t)-v^*+d, \tag{12}$$

$$\bar{w}(-l(t),t)=\frac{v^*-a\rho^*}{v^*}\bar{v}(-l(t),t). \tag{13}$$

We define $Y(-l(t),t) = v(-l(t),t)$ as the available measurement obtained from the real-time sensing. The main focus of this paper is to design an observer–based feedback controller for system (9)–(13) by utilizing the boundary measurement $Y(-l(t),t)$ to regulate the traffic flow state and the stop–and–go wave, and to reject actuator input disturbances. Hence, we will firstly design a moving boundary observer in the following section.

III. Observer Design

We employ the backstepping method to design a moving boundary observer to estimate the system states $v(x,t), w(x,t)$, by using the available boundary measurements only. The observer is built as a copy of the plant (9)–(10) with boundary error injections:

$$\hat{v}_t - (w^* - 2v^*)\hat{v}_x = \frac{v_f - \hat{w}}{\tau} + \Gamma_1(x,t)\left(Y(-l(t),t) - \hat{v}(-l(t),t)\right), \tag{14}$$

$$\hat{w}_t + v^*\hat{w}_x = \frac{v_f - \hat{w}}{\tau} + \Gamma_2(x,t)\left(Y(-l(t),t) - \hat{v}(-l(t),t)\right), \tag{15}$$

$$\hat{v}(0,t) = U(t) - v^* + d, \tag{16}$$

$$\hat{w}(-l(t),t) = \frac{v^* - a\rho^*}{v^*} Y(-l(t),t), \tag{17}$$

where $\hat{v}, \hat{\rho}, \hat{w}$ denote the state estimates of v, ρ, w respectively, and $\Gamma_1(x,t), \Gamma_2(x,t)$ are the observer gains.

Recalling (9)–(13) and (14)–(17), denote the observer errors as $\tilde{v}(x,t) = v(x,t) - \hat{v}(x,t)$, $\tilde{w}(x,t) = w(x,t) - \hat{w}(x,t)$, and then the resulting observer error dynamics are given by

$$\tilde{v}_t - (w^* - 2v^*)\tilde{v}_x = -\frac{\tilde{w}}{\tau} - \Gamma_1(x,t)\tilde{v}(-l(t),t), \tag{18}$$

$$\tilde{w}_t + v^*\tilde{w}_x = -\frac{\tilde{w}}{\tau} - \Gamma_2(x,t)\tilde{v}(-l(t),t), \tag{19}$$

$$\tilde{v}(0,t) = 0, \tag{20}$$

$$\tilde{w}(-l(t),t) = 0. \tag{21}$$

Using the backstepping method to map the system (18)–(21) to the target observer error system, whose exponential stability results can be obtained directly, thus obtaining the observer gains $\Gamma_1(x,t), \Gamma_2(x,t)$ that guarantee the exponential stability of the system (18)–(21).

According to [13], apply the backstepping transformation

$$\tilde{v}(x,t) = \tilde{\alpha}(x,t) - \int_{-l(t)}^{x} \phi(x,y)\tilde{\alpha}(y,t)dy, \tag{22}$$

$$\tilde{w}(x,t) = \tilde{\beta}(x,t) - \int_{-l(t)}^{x} \psi(x,y)\tilde{\alpha}(y,t)dy, \tag{23}$$

where kernels $\phi(x,y), \psi(x,y)$ are to be determined.

The target observer error system is set up as

$$\tilde{\alpha}_t - (w^* - 2v^*)\tilde{\alpha}_x = -\frac{1}{\tau}\tilde{\beta} + \int_{-l(t)}^{x} \tilde{M}(x,y)\tilde{\beta}(y,t)dy, \tag{24}$$

$$\tilde{\beta}_t + v^*\tilde{\beta}_x = \frac{1}{\tau}\tilde{\alpha} - \frac{1}{\tau}\tilde{\beta} + \int_{-l(t)}^{x} \tilde{N}(x,y)\tilde{\beta}(y,t)dy, \tag{25}$$

$$\tilde{\alpha}(0,t) = 0, \tag{26}$$

$$\tilde{\beta}(-l(t),t) = 0, \tag{27}$$

where $\tilde{M}(x,y), \tilde{N}(x,y)$ are the integral operator kernels.

By replacing the transformation of (22)–(23) with (18) and inserting (24), through a lengthy computation, we can obtain

$$\begin{aligned}
&\tilde{v}_t - (w^* - 2v^*)\tilde{v}_x + \frac{\tilde{w}}{\tau} + \Gamma_1(x,t)\tilde{v}(-l(t),t) \\
&= \int_{-l(t)}^{x} [(w^* - 2v^*)\phi_y(x,y) + (w^* - 2v^*)\phi_x(x,y) \\
&\quad - \frac{1}{\tau}\psi(x,y)]\tilde{\alpha}(y,t)dy + \int_{-l(t)}^{x} [\tilde{M}(x,y) + \frac{1}{\tau}\phi(x,y) \\
&\quad - \int_{y}^{x} \phi(x,z)\tilde{M}(z,y)dz]\tilde{\beta}(y,t)dy + [(w^* - 2v^*)\phi(x,-l(t)) \\
&\quad - \dot{l}(t)\phi(x,-l(t)) + \Gamma_1(x,t)]\tilde{\alpha}(-l(t),t).
\end{aligned} \tag{28}$$

By replacing the transformation of (22)–(23) with (19) and inserting (25), through a lengthy computation, we can obtain

$$\begin{aligned}
&\tilde{w}_t + v^*\tilde{w}_x + \frac{\tilde{w}}{\tau} + \Gamma_2(x,t)\tilde{v}(-l(t),t) \\
&= [\frac{1}{\tau} + (v^* - w^*)\psi(x,x)]\tilde{\alpha}(x,t) + \int_{-l(t)}^{x} [(w^* - 2v^*)\psi_y(x,y) \\
&\quad - v^*\psi_x(x,y) - \frac{1}{\tau}\psi(x,y)]\tilde{\alpha}(y,t)dy + \int_{-l(t)}^{x} [\tilde{N}(x,y) \\
&\quad + \frac{1}{\tau}\psi(x,y) - \int_{y}^{x} \psi(x,z)\tilde{M}(z,y)dz]\tilde{\beta}(y,t)dy + [\Gamma_2(x,t) \\
&\quad + (w^* - 2v^*)\psi(x,-l(t)) - \dot{l}(t)\psi(x,-l(t))]\tilde{\alpha}(-l(t),t).
\end{aligned} \tag{29}$$

To ensure that the right hand sides of equations (28)–(29) are all equal to zero, the kernels $\phi(x,y), \psi(x,y)$ should satisfy

$$\phi_y(x,y) + \phi_x(x,y) - \frac{1}{\tau(w^* - 2v^*)}\psi(x,y) = 0, \tag{30}$$

$$(w^* - 2v^*)\psi_y(x,y) - v^*\psi_x(x,y) - \frac{1}{\tau}\psi(x,y) = 0, \tag{31}$$

$$\phi(0,y) = 0, \tag{32}$$

$$\psi(x,x) = \frac{1}{(w^* - v^*)\tau}, \tag{33}$$

and the integral operator kernels $\tilde{M}(x,y), \tilde{N}(x,y)$ should satisfy

$$\tilde{M}(x,y) = -\frac{1}{\tau}\phi(x,y) + \int_{y}^{x} \phi(x,z)\tilde{M}(z,y)dz, \tag{34}$$

$$\tilde{N}(x,y) = -\frac{1}{\tau}\psi(x,y) + \int_{y}^{x} \psi(x,z)\tilde{M}(z,y)dz. \tag{35}$$

Thus, the observer gains $\Gamma_1(x,t), \Gamma_2(x,t)$ can be obtained

$$\Gamma_1(x,t) = -(w^* - 2v^*)\phi(x,-l(t)) - \dot{l}(t)\phi(x,-l(t)), \tag{36}$$

$$\Gamma_2(x,t) = -(w^* - 2v^*)\psi(x,-l(t)) - \dot{l}(t)\psi(x,-l(t)). \tag{37}$$

Lemma 1: *The kernel equations (30)–(33) have a unique continuous solution* $(\phi(x,y), \psi(x,y))$ *in the triangular domain* $D_1 = \{(x,y) | -l(t) \le y \le x \le 0\}$.

Proof: The equation set (30)–(33) belongs to a general class of kernel equations in the same form, whose well–posedness is proved in [14] and [15]. Thus Lemma 1 can be proved with details omitted in this paper. □

Due to the invertibility of the transformation in (22)–(23), the stability of the target observer error system $(\tilde{\alpha}(x,t),\tilde{\beta}(x,t))$ and the stability of the observer error system $(\tilde{v}(x,t),\tilde{w}(x,t))$ are equivalent. Next, we apply Lyapunov analysis to prove the exponential stability of the observer error dynamics (18)–(21) by equivalently considering the stability of system (36)–(37).

Theorem 1: *Considering the observer error system (18)–(21) with observer gains (36)–(37) for initial observer error states* $(\tilde{v}(x,t_0),\tilde{w}(x,t_0)) \in H^1((-l_0,0);\mathbb{R})$*, the observer error is uniformly exponentially stable.*

Proof: Firstly, we establish the stability proof for the target observer error system (24)–(27) w.r.t. $(\tilde{\alpha}(x,t),\tilde{\beta}(x,t))$ with the same structure as the exponentially stable target system in [13]. Therefore, the target observer error system would be exponentially stable. The Lyapunov function V_1 for the system (24)–(27) is defined as $V_1 : H^1((-l(t),0),\mathbb{R}^2) \to \mathbb{R}$,

$$V_1(t) = \frac{d_2}{2}\int_{-l(t)}^{0} e^{\delta_2 x}\tilde{\alpha}_x^2(x,t)dx + \frac{c_2}{2}\int_{-l(t)}^{0} e^{-\delta_2 x}\tilde{\beta}_x^2(x,t)dx + \frac{d_1}{2}\int_{-l(t)}^{0} e^{\delta_1 x}\tilde{\alpha}^2(x,t)dx + \frac{c_1}{2}\int_{-l(t)}^{0} e^{-\delta_1 x}\tilde{\beta}^2(x,t)dx \tag{38}$$

where positive parameters $c_i, d_i, \delta_i, i=1,2$ are to be chosen.

Define $\Omega_1(t) = ||\tilde{\alpha}(x,t)||^2_{H^1((-l_0,0);\mathbb{R})} + ||\tilde{\beta}(x,t)||^2_{H^1((-l_0,0);\mathbb{R})}$, and there exist two positive constants θ_1,θ_2 such that $\theta_1\Omega_1(t) \le V_1(t) \le \theta_2\Omega_1(t)$. Taking the derivative of $V_1(t)$ along (24)–(27), and considering the propagation velocity of the stop–and–go wave $-\dot{l}(t)$ is bounded, i.e. $|-\dot{l}(t)| < \min\{|v^*|,|w^*-2v^*|\}$, then using Young's inequality and Cauchy–Schwarz inequality, and through a lengthy calculation, we have

$$\begin{aligned}\dot{V}_1(t) \le& -(c_1\delta_1\xi_2 + c_1\xi_2 + d_1\xi_2 - c_1\xi_1 - \frac{c_1}{\delta_1}\xi_1 - \frac{d_1}{\delta_1}\xi_2 - d_2\xi_1 - \frac{d_2}{\delta_2}\xi_1 + d_2\xi_2 - \frac{c_2}{\delta_2}\xi_1 - c_2\xi_1)\int_{-l(t)}^{0}\tilde{\beta}^2(x,t)dx \\ &- (d_1\delta_1\xi_4 + d_1\xi_4 - c_1\xi_3 - d_1\xi_3)\int_{-l(t)}^{0}\tilde{\alpha}^2(x,t)dx - (c_2\xi_4 + c_2\delta_2\xi_4 + d_2\xi_4 - c_2\xi_3)\int_{-l(t)}^{0}\tilde{\beta}_x^2(x,t)dx - (d_2\xi_4 - d_2\xi_3 \\ &+ d_2\delta_2\xi_4)\int_{-l(t)}^{0}\tilde{\alpha}_x^2(x,t)dx - \left(\frac{d_2(w^*-2v^*)}{2} - \frac{d_2}{2}\dot{l}(t) - c_2\xi_3\right)\tilde{\alpha}_x^2(-l(t),t) - (c_1\xi_4 - d_2\xi_3)\tilde{\beta}^2(0,t) - \frac{c_2v^*}{2}\tilde{\beta}_x^2(0,t) \\ &- \frac{d_1}{2}e^{-\delta L}\left(w^*-2v^*-\dot{l}(t)\right)\tilde{\alpha}^2(-l(t),t),\end{aligned} \tag{39}$$

where $\kappa_i, i=1,2,3,4,5,6,7,8,9,10$ are positive constants,

$$\xi_1 = \max\left\{\frac{e^{\delta_1 L}}{2\tau\kappa_1}, \frac{\bar{N}\kappa_2 e^{\delta_1 L}}{2}, \frac{\bar{N}(e^{\delta_1 L}-1)}{2\kappa_2}, \frac{e^{\delta_1 L}\kappa_1}{2\tau}, \frac{\bar{M}}{2\kappa_5}, \frac{\bar{M}^2}{2(w^*-2v^*)}, \frac{\bar{M}_x}{2\kappa_6}(1-e^{-\delta_2 L}), \frac{\bar{N}_x}{2\kappa_9}(e^{\delta_2 L}-1), \frac{\bar{N}}{2\kappa_{10}}e^{\delta_2 L}\right\}, \tag{40}$$

$$\xi_2 = \min\left\{\frac{v^*}{2}, \frac{\bar{M}}{2\tau\kappa_3}(1-e^{-\delta_1 L}), \frac{e^{-\delta_1 L}}{2\tau\kappa_1}, \frac{\bar{M}^2}{2\kappa_7(w^*-2v^*)}\right\}, \tag{41}$$

$$\xi_3 = \max\left\{\frac{\kappa_1}{2\tau}e^{\delta_1 L}, \frac{\bar{M}\kappa_2}{2}, \frac{\kappa_8}{2\tau}e^{\delta_2 L}, \frac{\bar{N}_x\kappa_9}{2}e^{\delta_2 L}, \frac{\bar{N}\kappa_{10}}{2}e^{\delta_2 L}, \frac{\kappa_5\bar{M}}{2}, \frac{\kappa_6\bar{M}_x}{2}, \frac{e^{\delta_2 L}}{2\kappa_8\tau}, \frac{1-\kappa_7}{2(w^*-2v^*)}\right\}, \tag{42}$$

$$\xi_4 = \min\left\{\frac{w^*-2v^*}{2}e^{-\delta_1 L}, \frac{\kappa_1}{2\tau}e^{-\delta_1 L}, \frac{v^*}{2}, \frac{1}{\tau}, \frac{e^{-\delta_2 L}}{2\tau\kappa_4}, \frac{w^*-2v^*}{2}e^{-\delta_2 L}, \frac{\kappa_4}{2\tau}e^{-\delta_2 L}\right\}, \tag{43}$$

$$\bar{N} = \max_{-L\le y\le x\le 0}\{|\tilde{N}(x,y)|\}, \bar{N}_x = \max_{-L\le y\le x\le 0}\{|\tilde{N}_x(x,y)|\}, \tag{44}$$

$$\bar{M} = \max_{-L\le y\le x\le 0}\{|\tilde{M}(x,y)|\}, \bar{M}_x = \max_{-L\le y\le x\le 0}\{|\tilde{M}_x(x,y)|\}. \tag{45}$$

Choosing parameters $c_1, d_1, c_2, d_2, \delta_1\delta_2$ to satisfy

$$\eta_1 = c_1\delta_1\xi_2 + c_1\xi_2 + d_1\xi_2 - c_1\xi_1 - \frac{c_1}{\delta_1}\xi_1 - \frac{d_1}{\delta_1}\xi_2 \tag{46}$$

$$- d_2\xi_1 - \frac{d_2}{\delta_2}\xi_1 + d_2\xi_2 - \frac{c_2}{\delta_2}\xi_1 - c_2\xi_1 > 0, \tag{47}$$

$$\eta_2 = d_1\delta_1\xi_4 + d_1\xi_4 - c_1\xi_3 - d_1\xi_3 > 0, \tag{48}$$

$$\eta_3 = c_2\delta_2\xi_4 + c_2\xi_4 + d_2\xi_4 - c_2\xi_3 > 0, \tag{49}$$

$$\eta_4 = d_2\delta_2\xi_4 + d_2\xi_4 - d_2\xi_3 > 0, \tag{50}$$

$$\eta_5 = \frac{d_2(w^*-2v^*)}{2} - \frac{d_2}{2}\dot{l}(t) - c_2\xi_3 > 0, \tag{51}$$

$$\eta_6 = c_1\xi_4 - d_2\xi_3 > 0. \tag{52}$$

Then, let $\sigma_1 = \min\{\eta_1,\eta_2,\eta_3,\eta_4,\}$, we thus obtain

$$\begin{aligned}\dot{V}(t) \le& -\sigma_1 V(t) - \eta_6\tilde{\beta}^2(0,t) - \frac{d_1e^{-\delta_1 L}}{2}(w^*-2v^* - \dot{l}(t))\tilde{\alpha}^2(-l(t),t) - \eta_5\tilde{\alpha}_x^2(-l(t),t) - \frac{c_2v^*}{2}\tilde{\beta}_x^2(0,t) \\ \le& -\sigma_1 V(t).\end{aligned} \tag{53}$$

Therefore, we obtain the exponential stability of the target observer error system $(\tilde{\alpha}(x,t),\tilde{\beta}(x,t))$ in the sense of $\Omega_1(t)$. Due to the invertibility of the transformations (22)–(23), the exponential stability of the observer error system $(\tilde{v}(x,t),\tilde{w}(x,t))$ is proved. □

IV. Output Feedback Controller Design

In this section, we design output feedback control controller $U(t)$ by using the states recovered from the observer (14)–(17) via the backstepping method.

According to [16], using the backstepping transformation

$$\alpha(x,t) = \hat{v}(x,t) - \int_{-l(t)}^{x}\bar{\phi}(x,y)\hat{v}(y,t)dy - \int_{-l(t)}^{x}\bar{\psi}(x,y)\hat{w}(y,t)dy - \bar{\gamma}(x)(-\hat{l}(t)), \tag{54}$$

$$\beta(x,t) = \hat{w}(x,t). \tag{55}$$

We would like to convert the observer system (14)–(17) to the following target system $(\alpha(x,t),\beta(x,t))$:

$$\alpha_t = (w^*-2v^*)\alpha_x - \frac{1}{2\tau}\beta - J(x,t)\tilde{v}(-l(t),t), \tag{56}$$

$$\beta_t = -v^*\beta_x - \frac{1}{\tau}\alpha - \frac{1}{\tau}\beta + \Gamma_2(x,t)\tilde{v}(-l(t),t) + \frac{1}{\tau}\int_{-l(t)}^{x}\breve{\psi}(x,y)\beta(y,t)dy + \frac{1}{\tau}\breve{\gamma}(x)(-\hat{l}(t)) + \frac{1}{\tau}\int_{-l(t)}^{x}\breve{\phi}(x,y)\alpha(y,t)dy, \quad (57)$$

$$-\dot{\hat{l}}(t) = A(-\hat{l}(t)) + \frac{w^*}{2v^*}\alpha(-l(t),t), \quad (58)$$

$$\alpha(0,t) = k_i\int_0^t \beta(0,s) - \alpha(0,s)ds + d, \quad (59)$$

$$\beta(-l(t),t) = 0, \quad (60)$$

where $J(x,t) = \int_{-l(t)}^{x}[\bar{\phi}(x,y)\Gamma_1(y,t) + \bar{\psi}(x,y)\Gamma_2(y,t)]dy - \Gamma_1(x,t)$, A is Hurwitz constant coefficient, $k_i \in \mathbb{R}$ is an integral tuning parameter. $\breve{\phi}(x,y), \breve{\psi}(x,y), \breve{\gamma}(x)$ are kernels of the inverse transformations

$$\hat{v}(x,t) = \alpha(x,t) - \int_{-l(t)}^{x}\breve{\phi}(x,y)\alpha(y,t)dy - \int_{-l(t)}^{x}\breve{\psi}(x,y)\beta(y,t)dy - \breve{\gamma}(x)(-\hat{l}(t)), \quad (61)$$

$$\hat{w}(x,t) = \beta(x,t). \quad (62)$$

Substituting the transformations (54)–(55) into (56), therefor the kernels $\bar{\phi}(x,y), \bar{\psi}(x,y), \bar{\gamma}(x)$ in $D_2 = \{(x,y)| -l(t) \le y \le x \le 0\}$ should satisfy

$$(w^*-2v^*)\bar{\psi}_x(x,y) + v^*\bar{\psi}_y(x,y) + \frac{1}{\tau}(\bar{\phi}(x,y) + \bar{\psi}(x,y)) = 0, \quad (63)$$

$$(w^*-2v^*)\bar{\phi}_x(x,y) + (w^*-2v^*)\bar{\phi}_y(x,y) = 0, \quad (64)$$

$$\bar{\psi}(x,x) = \frac{1}{2\tau(w^*-3v^*)}, \quad (65)$$

$$(w^*-2v^*)(\bar{\phi}(x,-l(t)) - (1+\frac{w^*}{2v^{*2}}\tilde{v}(-l(t),t))\bar{\psi}(x,-l(t))) - \frac{w^*}{2v^*}\bar{\gamma}(x) + (-\hat{l}(t))(\frac{w^*}{2v^*}\bar{\gamma}(-l(t)) - A)(-\bar{\phi}(x,-l(t)) + \frac{w^*-2v^*}{v^*}\bar{\psi}(x,-l(t))) = 0, \quad (66)$$

$$\bar{\phi}(x,-l(t)) - \frac{w^*-2v^*}{v^*}\bar{\psi}(x,-l(t) = 0, \quad (67)$$

$$\frac{w^*}{2v^{*2}}(-\hat{l}(t))\bar{\gamma}(-l(t)) - \frac{1}{v^*}(-\hat{l}(t))A - 1 = 0, \quad (68)$$

$$(w^*-2v^*)\dot{\bar{\gamma}}(x) + (\frac{w^*}{2v^*}\bar{\gamma}(-l(t)) - A)\bar{\gamma}(x) = 0, \quad (69)$$

Lemma 2: *The kernel equations (63)–(69) have a unique continuous solution $(\bar{\phi}(x,y), \bar{\psi}(x,y), \bar{\gamma}(x))$ in the triangular domain $D_2 = \{(x,y)| -l(t) \le y \le x \le 0\}$.*

Proof: The kernel equations (63)-(69) have the same form as the kernel equations in [17]. Because the well–posedness has been proved in [17], Lemma 2 can be proved with details omitted in this paper. □

Considering the boundary condition (59) in the target system, the boundary condition (16) in the observer, and the transformation (54), we derive the controller as:

$$U(t) = v^* + k_i\int_0^t(\hat{w}(0,s) - \hat{v}(0,s))ds + \bar{\gamma}(0)(-\hat{l}(t)) + \int_{-l(t)}^{0}\bar{\phi}(0,y)\hat{v}(y,t)dy + \int_{-l(t)}^{0}\bar{\psi}(0,y)\hat{w}(y,t)dy + k_i\int_0^t\bar{\gamma}(0)(-\hat{l}(s))ds + k_i\int_0^t\int_{-l(t)}^{0}\bar{\phi}(0,y)\hat{v}(y,s)dyds + k_i\int_0^t\int_{-l(t)}^{0}\bar{\psi}(0,y)\hat{w}(y,s)dyds. \quad (70)$$

Theorem 2: *If initial values $(\hat{v}(x,t_0), \hat{w}(x,t_0)) \in H^1((-l_0,0);\mathbb{R})$ and $l_0 \in (-L,0)$, the observer system (14)–(17) under the controller (70) is exponentially stable.*

Proof: We establish the stability proof of the target system $(\alpha(x,t), \beta(x,t))$ (56)–(60) via Lyapunov method. Due to the invertibility of the backstepping transformation (54)–(55), the stability of the target system is equivalent to that of the observer system $(\hat{v}(x,t), \hat{w}(x,t))$ (14)–(17). The Lyapunov function $V_2 : H^1((-l(t),0),\mathbb{R}^2) \to \mathbb{R}$ for the system (56)–(60) is defined as

$$V_2(t) = (-\hat{l}(t))^\top P_1(-\hat{l}(t)) + \alpha(0,t)^\top P_2\alpha(0,t) + \frac{d_2}{2}\int_{-l(t)}^{0}e^{\delta_3 x}\alpha^2(x,t)dx + \frac{c_2}{2}\int_{-l(t)}^{0}e^{-\delta_3 x}\beta^2(x,t)dx + \frac{d_4}{2}\int_{-l(t)}^{0}e^{\delta_4 x}\alpha_x^2(x,t)dx + \frac{c_4}{2}\int_{-l(t)}^{0}e^{-\delta_4 x}\beta_x^2(x,t)dx, \quad (71)$$

where the scalar $P_1 = P_1^\top > 0$ is the solution to the Lyapunov equation $P_1A + A^\top P_1 = -Q_1$, for $Q_1 = Q_1^\top > 0$, and the positive parameters P_2, d_2, c_2, δ_2 are to be chosen later. Defining $\Omega_2(t) = ||\alpha||^2_{H^1((-l_0,0);\mathbb{R})} + ||\beta||^2_{H^1((-l_0,0);\mathbb{R})} + |(-\hat{l}(t))|^2$, there exist two positive constants θ_3, θ_4 holding $\theta_3\Omega_2(t) \le V_2(t) \le \theta_4\Omega_2(t)$. Analogous to the proof of Theorem 1, taking the derivative of $V_2(t)$ along (56)–(60), using Young's inequality and Cauchy–Schwarz inequality, we obtain that $\dot{V}_2(t)$ is negative, the details of which are omitted in this paper. Therefore, we obtain the exponential stability result in the sense of $\Omega_2(t)$. Due to the invertibility of the transformations (54)–(55), the exponential stability of the observer system $(\hat{v}(x,t), \hat{w}(x,t))$ is proved. □

Theorem 3: *Considering the plant (9)–(13), with the observer (14)–(17), and the controller (70), for any initial values $(\bar{v}(x,t_0), \bar{w}(x,t_0), \hat{v}(x,t_0), \hat{w}(x,t_0)) \in L^2(-L_0,0)$, $l_0 \in (-L,0)$, the closed–loop system is uniformly exponentially stable.*

Proof: Recalling the exponential stability result in the sense of $||\hat{v}(\cdot,t)||^2_{H^1((-l_0,0);\mathbb{R})} + ||\hat{w}(\cdot,t)||^2_{H^1((-l_0,0);\mathbb{R})} + |-\hat{l}(t)|^2$ proved in Theorem 2, and the exponential stability result in the sense of $||\tilde{v}(\cdot,t)||^2_{H^1((-l_0,0);\mathbb{R})} + ||\tilde{w}(\cdot,t)||^2_{H^1((-l_0,0);\mathbb{R})}$ proved in Theorem 1, we obtain the exponential stability result in the sense of $||\bar{v}(\cdot,t)||^2_{H^1((-l_0,0);\mathbb{R})} + ||\bar{w}(\cdot,t)||^2_{H^1((-l_0,0);\mathbb{R})} + |-\hat{l}(t)|^2$. The proof of Theorem 3 is completed. □

V. Simulation

The numerical simulation is performed by the finite-difference method for the discretization in time and space

TABLE I

TRAFFIC PARAMETERS AND STEADY–STATES IN THE SIMULATION.

Parameters	Values	Unit
L	2	km
l_0	1.5	km
ρ^*	100	veh/km
v^*	45	km/hr
ρ_m	160	veh/km
v_f	120	km/hr
a	0.75	km^2/veh/hr
τ	60	s

after converting the time–varying domain PDE to a fixed domain PDE via introducing $\varsigma = \frac{x}{l(t)}$. The solutions of the kernel equations (30)–(33) and (63)–(69), which are coupled linear hyperbolic PDEs, are also solved by the finite–difference method.

The steady–states and some traffic parameters of the road are shown in Table I. The parameters chosen here are $k_i = 20$, and the initial conditions are given as $\bar{v}(\varsigma, 0) = -7.5\cos(8.5\pi\varsigma)$, $\bar{\rho}(\varsigma, 0) = -5.0\sin(1.14\pi\varsigma)$. To compute the numerical solutions of system $(\bar{v}(x,t), \bar{w}(x,t))$ (9)–(13) and system $(\hat{v}(x,t), \hat{w}(x,t))$ (14)–(17), we discretize them by using the two–step variant of Lax–Wendroff method.

Fig. 2 show the evolution of $-l(t), -\dot{l}(t)$ with two different disturbances $d = 1.5$ km/hr and 5.0 km/hr, respectively. Figs. 3 and Fig. 4 show the evolution of $(\bar{v}, \bar{\rho})$, $(\hat{v}, \hat{\rho})$ with disturbances $d = 1.5$ km/hr in congestion regime, respectively. The highlighted blue and red lines represent the initial values and the evolution of boundary, respectively. It is observed that, after around 0.3 hour, all of them asymptotically converge to zero using the designed controller $U(t)$, as expected from Theorem 3.

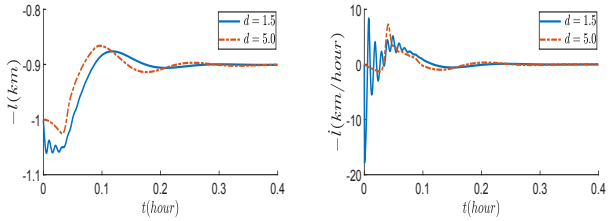

Fig. 2. The evolution of $-l(t)$ and $-\dot{l}(t)$.

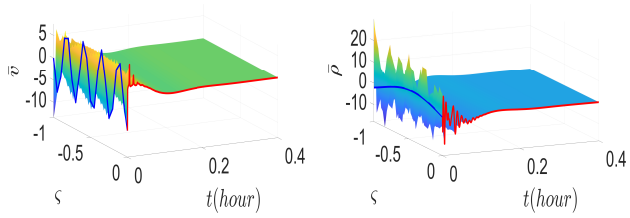

Fig. 3. The evolution of v and ρ.

VI. CONCLUSION

In this paper, we consider the stabilization problem of traffic flow state with stop–and–go waves and unknown perturbation over a time–varying moving spatial domain in the congestion regime. Based on the ARZ traffic flow model, a novel propagation model of stop–and–go waves is established. Using the PDE backstepping method, we construct an observer–based output feedback controller. The exponential stability is proved via Lyapunov analysis. Our future work would be developing adaptive controllers for the ARZ model in the moving spatial domain.

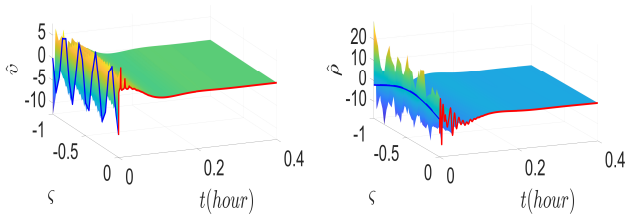

Fig. 4. The evolution of observer $\hat{v}$ and $\hat{\rho}$.

REFERENCES

[1] B. S. Kerner. *Introduction to modern traffic flow theory and control*. Springer Berlin Heidelberg, 2009.

[2] Y. Sugiyama, M. Fukui, M. Kikuchi, K. Hasebe, A. Nakayama, K. Nishinari, S. Tadaki, and S. Yukawa. Traffic jams without bottlenecks–experimental evidence for the physical mechanism of the formation of a jam. *New Journal of Physics*, 10:033001, 03 2008.

[3] H. M. Zhang. A non-equilibrium traffic model devoid of gas-like behavior. *Transportation Research Part B*, 36(3):275–290, 2002.

[4] H. Yu and M. Krstic. Output feedback control of two-lane traffic congestion. *Automatica*, 125:109379, 2021.

[5] M. Burkhardt, H. Yu, and M. Krstic. Stop-and-go suppression in two-class congested traffic. *Automatica*, 125:109381, 2021.

[6] L. Guan, L. Zhang, and C. Prieur. Optimal observer-based output feedback controller for traffic congestion with bottleneck. *International Journal of Robust and Nonlinear Control*, 31(15):7087–7106, 2021.

[7] L. Zhang and Y. Lu. Distributed consensus-based boundary observers for freeway traffic estimation with sensor networks. In *2020 American Control Conference (ACC)*, pages 4497–4502, 2020.

[8] H. Yu, A.M. Bayen, and M. Krstic. Boundary observer for congested freeway traffic state estimation via aw-rascle-zhang model. *IFAC-PapersOnLine*, 52(2):183–188, 2019.

[9] H. Yu, M. Diagne, L. Zhang, and M. Krstic. Bilateral boundary control of moving shockwave in LWR model of congested traffic. *IEEE Transactions on Automatic Control*, 66(3):1429–1436, 2021.

[10] H. Luan, J. Zhan, and L. Zhang. Moving boundary observer for traffic state estimation with shock waves. *The 22nd World Congress of the International Federation of Automatic Control (IFAC World Congress)*, Accepted, 2023.

[11] B. D. Greenshields. A study of traffic capacity. In *Proceedings of the Highway Research Board*, pages 448–477, 1935.

[12] A. Bressan. *Hyperbolic systems of conservation laws: the one-dimensional Cauchy problem*, volume 20. Oxford University Press, USA, 2000.

[13] J. Wang and M. Krstic. Delay-compensated event-triggered boundary control of hyperbolic pdes for deep-sea construction. *Automatica*, 138:110137, 2022.

[14] R. Vazquez, M. Krstic, and J.M. Coron. Backstepping boundary stabilization and state estimation of a 2 × 2 linear hyperbolic system. In *2011 50th IEEE Conference on Decision and Control and European Control Conference*, pages 4937–4942, 2011.

[15] L. Hu, F. Di Meglio, R. Vazquez, and M. Krstic. Control of homodirectional and general heterodirectional linear coupled hyperbolic pdes. *IEEE Transactions on Automatic Control*, 61(11):3301–3314, 2016.

[16] J. Wang, Y. Pi, and M. Krstic. Balancing and suppression of oscillations of tension and cage in dual–cable mining elevators. *Automatica*, 98:223–238, 2018.

[17] F. Di Meglio, F. Bribiesca Argomedo, L. Hu, and M. Krstic. Stabilization of coupled linear heterodirectional hyperbolic pde-ode systems. *Automatica*, 87:281–289, 2018.